

CrystEngComm

Accepted Manuscript



This is an *Accepted Manuscript*, which has been through the Royal Society of Chemistry peer review process and has been accepted for publication.

Accepted Manuscripts are published online shortly after acceptance, before technical editing, formatting and proof reading. Using this free service, authors can make their results available to the community, in citable form, before we publish the edited article. We will replace this *Accepted Manuscript* with the edited and formatted *Advance Article* as soon as it is available.

You can find more information about *Accepted Manuscripts* in the [Information for Authors](#).

Please note that technical editing may introduce minor changes to the text and/or graphics, which may alter content. The journal's standard [Terms & Conditions](#) and the [Ethical guidelines](#) still apply. In no event shall the Royal Society of Chemistry be held responsible for any errors or omissions in this *Accepted Manuscript* or any consequences arising from the use of any information it contains.

COMMUNICATION

Simultaneous phase and size control in the synthesis of Cu_2SnS_3 and $\text{Cu}_2\text{ZnSnS}_4$ nanocrystals

Cite this: DOI: 10.1039/x0xx00000x

Youngrong Park, Ho Jin, Joonhyuck Park and Sungjee Kim*

Received 00th January 2012,
Accepted 00th January 2012

DOI: 10.1039/x0xx00000x

www.rsc.org/cystengcomm

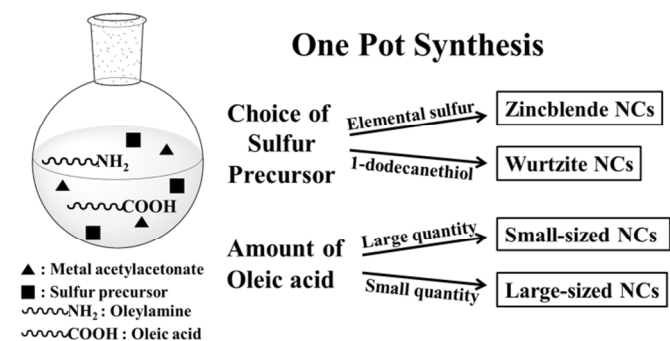
Facile and rapid one-pot synthesis for nearly monodisperse Cu_2SnS_3 and $\text{Cu}_2\text{ZnSnS}_4$ nanocrystals was developed using a heat-up method. Their crystalline phase and size were simultaneously controlled by judiciously choosing the sulfur precursor reactivity and the oleic acid content.

Copper-based ternary and quaternary semiconductors such as Cu_2InS_3 or $\text{Cu}(\text{In,Ga})\text{S}_2$ have been explored intensively as absorbing materials for thin-film photovoltaic devices. However indium and gallium are not widely available and relatively expensive, which may limit the practicality for device applications. Cu_2SnS_3 (CTS) and $\text{Cu}_2\text{ZnSnS}_4$ (CZTS) have emerged as an alternative that are composed of more earth-abundant elements. These semiconductors are promising for solar energy conversion materials due to the high optical absorption coefficient ($>10^4 \text{ cm}^{-1}$), cost-effectiveness, environmentally friendliness as being free of heavy metal ions, and suitable energy band gap ($\sim 1.5 \text{ eV}$).¹⁻³ Guo *et al.*⁴ reported the synthesis of the CZTS nanocrystals (NCs) and its use for an absorber layer. Synthetic protocols for CTS and CZTS NCs have been fiercely pursued, which includes hot injection strategy,³⁻⁵ one-pot synthesis,⁶ hydrothermal method,⁷⁻⁹ and microwave-assisted method¹⁰.

Controlling the phase, size, shape, and composition of NC is a prerequisite before the NC is fully realizing the potential for the optoelectronic devices. For example, photovoltaic performance of NC-based solar cells is greatly affected by the NC crystal structure, size, and composition.¹¹ Liu *et al.* have reported the zincblende and wurtzite CTS NCs by hot injection method, where the crystal phase was controlled by introducing different sulfur precursors.¹² In the case of CZTS NCs, the phase has been controlled by controlling the injection temperature.¹³ Chang *et al.* have reported the role of solvent, where coordinating oleylamine or non-coordinating octadecene solvent determined the phase (wurtzite or zincblende) of CTS or CZTS NCs.¹⁴ Recently, Zou *et al.* have reported the phase-controlled synthesis of CZTS by different reactivity of octadecene-sulfur.¹⁵ Orthorhombic⁷, wurtzite^{1,5,6,13} and kesterite CZTS³ have

been reported using various synthetic routes that include hydrothermal and heat-up methods. Great interest has been attracted also to the size control of CTS and CZTS NCs. Khare *et al.* have demonstrated the size control of CZTS NCs ranging from 2 to 7 nm in diameter by varying the oleylamine amount and the reaction temperature.¹⁶ Liu *et al.* showed that the hydrothermal reaction time for the synthesis of CZTS NCs critically determined the NC size ranging from 3 to 10.5 nm.¹⁷ However, systematic and simultaneous control over the crystalline phase and size of CTS and CZTS NCs have been challenging. A simple synthetic protocol that can flexibly tune the crystalline phase and the size would greatly foster the development of NC-incorporated device applications. Herein, we report a simple and rapid one-pot synthesis that yields nearly monodisperse CTS or CZTS NCs. Their crystalline phase and size were tailored simultaneously by the choice of sulfur precursor and the oleic acid (OA) amount (See scheme 1).

For a typical CTS or CZTS NC synthesis, stoichiometric amounts of metal acetylacetonates were mixed with elemental sulfur (ES) or 1-dodecanethiol (DDT) in oleylamine. OA was added to the mixture flask, and the flask was purged with nitrogen and was heated up to 100 °C for the case of ES or to 240 °C for the DDT case. The heat-up



Scheme 1 Schematic for non-injection, one-pot synthesis of CTS or CZTS NCs. By choosing the sulfur precursor reactivity and by choosing the amount of oleic acid amount, the phase and size of NCs can be simultaneously controlled.

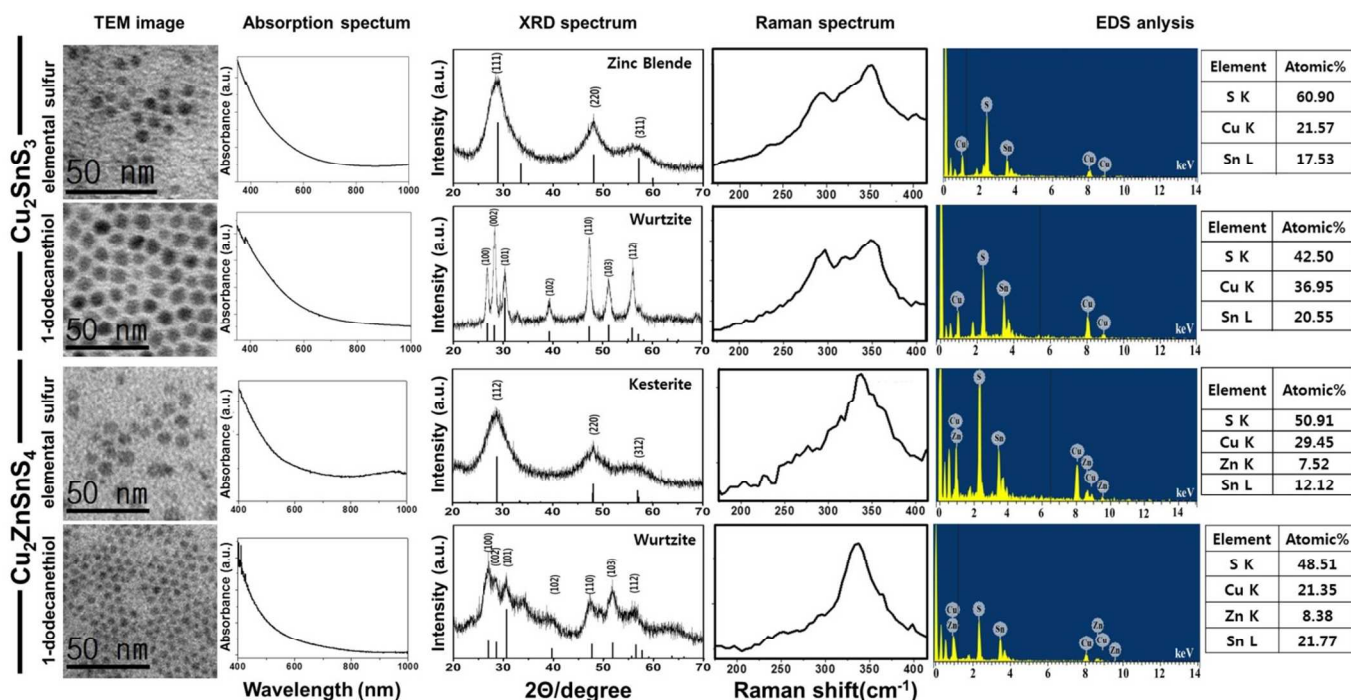


Fig. 1 TEM images, UV-vis absorption, XRD, Raman, and EDS spectra and the analysis for CTS NCs synthesized using elemental sulfur (top row), CTS NCs synthesized using 1-dodecanethiol (second row), CZTS NCs synthesized using elemental sulfur (third row), and CZTS NCs synthesized using 1-dodecanethiol (bottom row).

took 20 minutes, and the heating source was immediately removed after reaching the reaction temperature and the flask was cooled to room temperature. Detailed synthetic procedures can be found in Electronic Supplementary Information.

CTS and CZTS NCs were synthesized using either ES or DDT as the sulfur precursor. For the four cases of CTS-ES, CTS-DDT, CZTS-ES, and CZTS-DDT, transmission electron microscopy (TEM) images, absorption spectra, X-ray diffraction (XRD) spectra, Raman spectra, and energy dispersive spectroscopy (EDS) spectra were obtained (Fig. 1). The synthesized NCs were quasi-spherical and narrowly size-distributed with the relative monodispersity around 10%. The average NC diameters were 6.8 nm \pm 0.6 nm (CTS-ES), 9.3 nm \pm 1.3 nm (CTS-DDT), 9.2 nm \pm 1.2 nm (CZTS-ES), and 4.9 nm \pm 0.5 nm (CZTS-DDT) (See more TEM images at Fig. S1). UV-vis absorption spectra showed broad and featureless profiles with the tails extending to over 800 nm. The broad absorption profiles can be advantageous as light absorbers in photovoltaic device application. The choice of sulfur precursor critically determined the crystalline structure of the final NCs. CTS NCs of zinc-blende were obtained when ES was used, whereas DDT yielded wurtzite CTS NCs. The XRD patterns matched quite well with simulated XRD patterns. Because standard JCPDS XRD data were unavailable for most of the crystal structures, we have generated simulated XRD patterns for those crystals using a commercially available program Diamond (Crystal Impact, Bonn, Germany) with Rietveld refinement by MAUD program (INEL, Artenay, France). Crystal structure parameters used for the simulations were added in the Supporting Information (Fig. S2). Similarly, CZTS-ES showed kesterite structure^{2,3} while CZTS-DDT was wurtzite. Different reaction temperature was used for the ES and DDT (100 °C for ES and 240 °C for DDT), however temperature itself was not the major factor affecting the final crystal structure of NCs. As a control experiment, CTS-ES was synthesized at an elevated temperature up to 300 °C, but the product NCs were still zinc-blende (Fig. S3). For

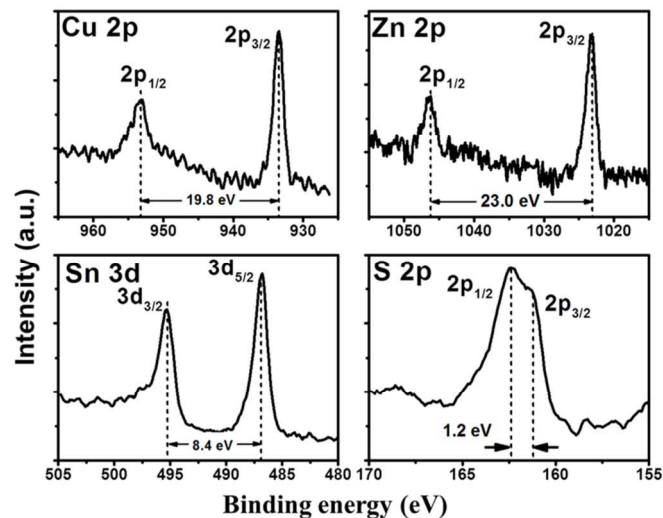


Fig. 2 X-ray photoelectron spectra of wurtzite CZTS NCs.

the CTS-DDT, no reaction proceeded at a temperature below 200 °C because DDT did not decompose. For a heat-up synthesis like ours, precursor reactivity seems to be more important than the final reaction temperature in determining the crystalline phase because the precursor reactivity plays a critical role in defining the temperature at the NC seed formation. ES is a more reactive sulfur precursor than DDT. CTS-ES forms the NC at a lower temperature than CTS-DDT, which can be easily observed by the color change. As the result, CTS-ES forms zincblende NCs which is known to favour lower temperature than wurtzite. Once the crystalline structure is determined at the NC seed stage, the structure does not change within the temperature range of our synthesis. For the four samples, Raman spectroscopy was performed to confirm the structure. The

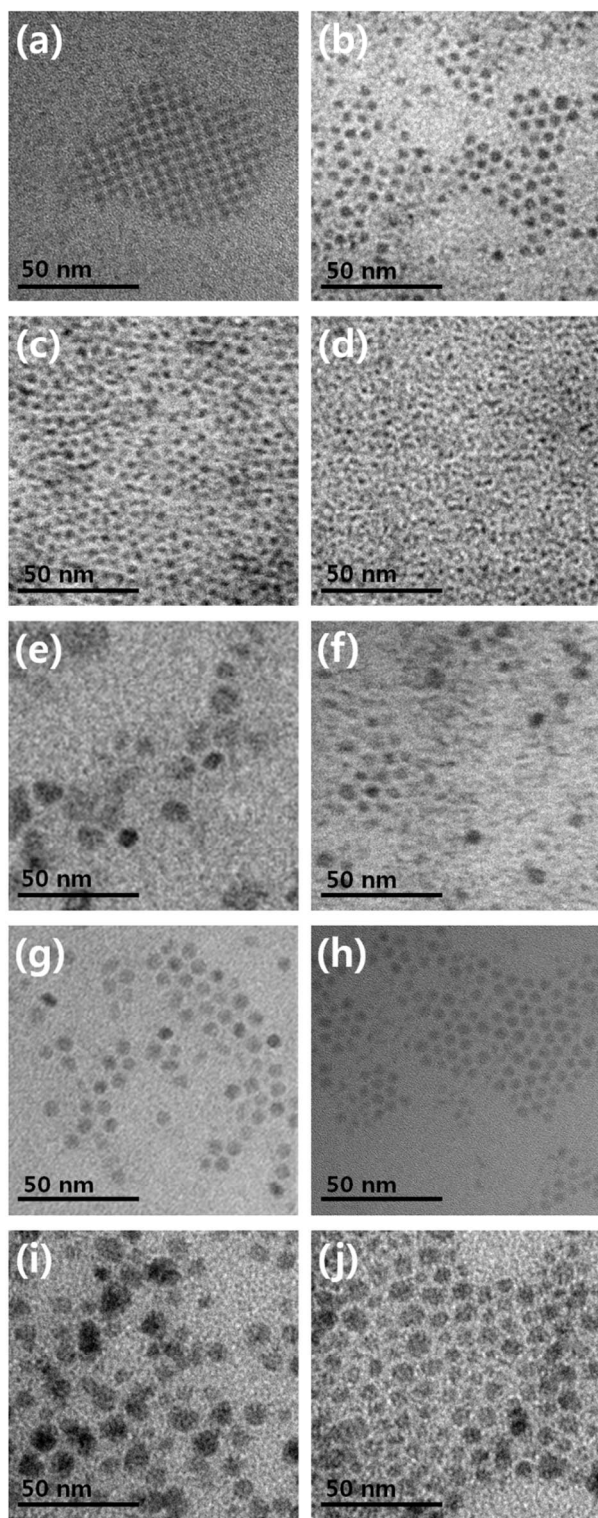


Fig. 3 TEM images of CTS NCs synthesized using DDT as the sulfur precursor as varying the oleic acid to cations molar ratio to 3:1 (a, average diameter 5.9 nm), 6:1 (b, 5.2 nm), 12:1 (c, 4.8 nm), and 18:1 (d, 3.2 nm). CTS NCs synthesized using ES with the ratio of 6:1 (e, 9.0 nm) and 18:1 (f, 6.8 nm). CZTS NCs synthesized using DDT with the ratio of 3:1 (g, 6.7 nm), 12:1 (h, 5.4 nm). CZTS NCs synthesized using ES with the ratio of 3:1 (i, 9.5 nm) and 6:1 (j, 7.3 nm).

peaks at the spectra were rather broad because of NC phonon confinement.¹⁷ CTS-ES and CTS-DDT showed two peaks at 294cm^{-1} , 353cm^{-1} and 296cm^{-1} , 348cm^{-1} , respectively, and CZTS-ES and

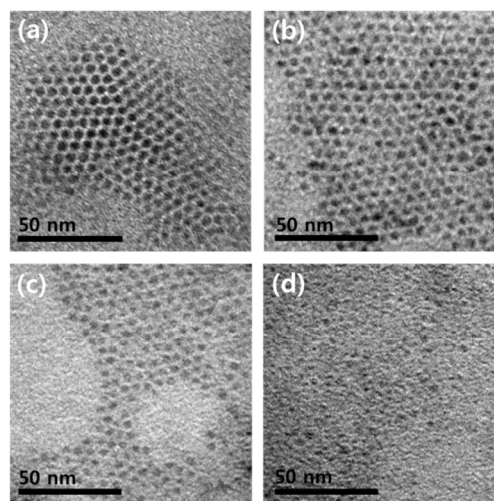


Fig. 4 TEM images of CTS aliquots using 1-dodecanethiol as the sulfur precursor that were collected when the color change occurred at 240°C . The sizes of nanocrystals are dependent on molar ratios of oleic acid to cation. (a) 3 : 1 ratio, 5.0 nm (b) 6 : 1 ratio, 4.8 nm (c) 12 : 1 ratio, 4.3 nm and (d) 18 : 1 ratio, 2.3 nm.

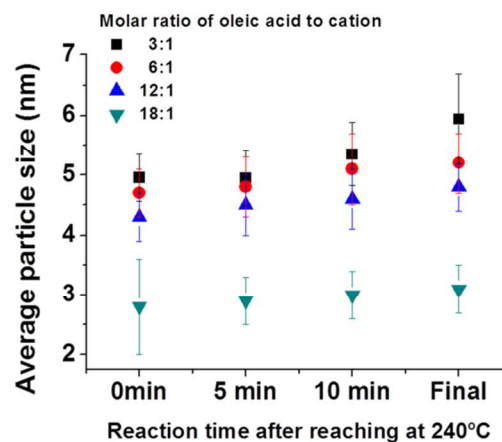


Fig. 5 Average particle size of CTS NC aliquots at the reaction time after reaching 240°C . The molar ratio of oleic acid to cations is 3:1 (black box), 6:1 (red circle), 12:1 (blue upright triangle), or 18:1 (green inverted triangle).

CZTS-DDT revealed single peak at 336cm^{-1} and 337cm^{-1} , respectively, which accorded well with the previous reports for CTS and CZTS.¹⁸ However, an additional Raman peak could be found at 320cm^{-1} for the case of wurtzite CTS, which might originate from co-existing orthorhombic Cu_3SnS_4 secondary phase.¹⁹ Strong (002), (110), and (112) wurtzite CTS XRD peaks also corroborates the secondary phase because the orthorhombic Cu_3SnS_4 (112), (220), and (132) reflect at the almost same angles (JCPDS 33-0501). Raman peaks at 315cm^{-1} and 355cm^{-1} that could originate from SnS_2 and ZnS were not observed. Composition of the NCs was determined by EDS, which verified the NCs contained all the expected constituent elements. However, the stoichiometry was not perfectly matched for CTS and CZTS (Fig. S4). The reasons could include non-perfect stoichiometry of NCs by defects or predominantly preferred surface crystalline facets, residual reactants such as ES, and unpurified by-products such as Cu_{2-x}S . X-ray photoelectron spectroscopy (XPS) analysis was performed to confirm the valence states of the wurtzite CZTS NCs (Fig. 2). Cu 2p peaks at 933.5 and 953.3 eV with the peak separation of 19.8 eV are characteristics of the splitting of Cu(I). So is Zn 2p peaks at 1023.4 and 1046.4 eV with the peak splitting of 23.0 eV for Zn(II), Sn 3d

peaks of 487.3 and 495.7 eV with the splitting of 8.3 eV for Sn(IV), and S 2p peaks at 161.2 and 162.4 eV with the splitting of 1.2 eV for the sulfide. This valence state represents that our synthetic route provides NCs with well-defined quaternary materials. Size control of the CTS and CZTS NCs was achieved by adjusting the OA amount (Fig. 3). For the CTS-DDT synthesis, the molar ratio of OA to cations was varied from 3:1 to 18:1 while fixing the total reaction volume by adjusting the oleylamine solvent, which yielded smaller NCs as increasing the OA ranging the NC size from about 6 to 3 nm. As increasing the OA ratio from 6 to 18 at CTS-ES syntheses, the size of NCs decreased from 9 to 7 nm. This tendency was also consistent to CZTS-ES and CZTS-DDT syntheses. OA activates metal salt precursors, and larger amount of OA can lead to smaller NC size as increasing the number of nuclei at the nucleation step. In addition, OA can also act as a growth-arresting stabilizing ligand to NCs. To confirm these two hypotheses, experiments for Fig 3a to d were repeated and aliquots were taken from the CTS-DDT reaction flask as soon as the color change occurred. For the OA ratio of 3, 6, 12, and 18, the average NC size was 5.0, 4.8, 4.3, and 2.3 nm, respectively (Fig. 4), which confirms the hypothesis of smaller nuclei. The growth was also followed by regularly taking out aliquots and measuring the size by TEM (Fig. 5), which confirmed the ligand role by revealing faster growth for smaller OA.

To summarize, a heat-up one-pot synthesis for CTS and CZTS NCs allowed simple and rapid control over the crystal structure and the size. The NCs are also readily dispersed in common organic solvents, which promises simple processes for device fabrications such as NC ink for thin-film solar cells.

This work was supported by Basic Science Research Program NRF-2013R1A1A2005582 and 2009-0094036 funded by the Ministry of Education, Science and Technology.

Notes and references

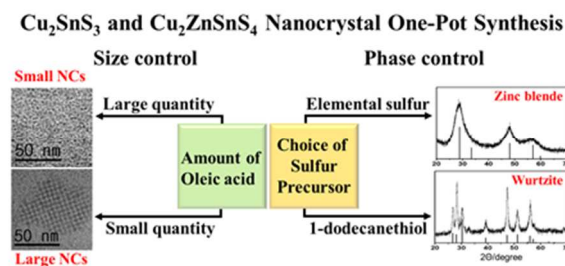
Department of Chemistry, Pohang University of Science and Technology (POSTECH), San 31, Hyojadong, Nam-gu, Pohang, 790-784, South Korea. E-mail: sungjee@postech.ac.kr

Electronic Supplementary Information (ESI) available: Detailed experimental procedures, additional TEM images and XRD pattern. See DOI: 10.1039/c000000x/

- X. Lu, Z. Zhuang, Q. Peng and Y. Li, *Chem. Commun.*, 2011, **47**, 3141-3143.
- C. Steinhagen, M. G. Panthani, V. Akhavan, B. Goodfellow, B. Koo and B. A. Korgel, *J. Am. Chem. Soc.*, 2009, **131**, 12554-12055.
- S. C. Riha, B. A. Parkinson and A. L. Prieto, *J. Am. Chem. Soc.*, 2009, **131**, 12054-12055.
- Q. Guo, H. W. Hillhouse and R. Agrawal, *J. Am. Chem. Soc.*, 2009, **131**, 11672-11673.
- A. Singh, H. Geaney, F. Lafir and K. M. Ryan, *J. Am. Chem. Soc.*, 2012, **134**, 2910-2913.
- M. Li, W.-H. Zhou, J. Guo, Y.-L. Zhou, Z.-L. Hou, J. Jiao, Z.-J. Zhou, Z.-L. Du and S.-X. Wu, *J. Phys. Chem. C*, 2012, **116**, 26507-26516.
- H. Jiang, P. Dai, Z. Feng, W. Fan and J. Zhan, *J. Mater. Chem.*, 2012, **22**, 7502-7506.
- M. Cao and Y. Shen, *J. Cryst. Growth*, 2011, **318**, 1117-1120.
- Y. L. Zhou, W. H. Zhou, Y. F. Du, M. Li and S. X. Wu, *Mater. Lett.*, 2011, **65**, 1535-1537.
- S. W. Shin, J. H. Han, C. Y. Park, A. V. Moholkar, J. Y. Lee and J. H. Kim *J. Alloys Compd.*, 2012, **516**, 96-101.
- M. G. Panthani, C. J. Stolle, D. K. Reid, D. J. Rhee, T. B. Harvey, V. A. Akhavan, Y. Yu and B. A. Korgel, *J. Phys. Chem. Lett.*, 2013, **4**, 2030-2034.
- Q. Liu, Z. Zhao, Y. Lin, P. Guo, S. Li, D. Pan and X. Ji, *Chem. Commun.*, 2011, **47**, 964-966

- C. A. Cattley, C. Cheng, S. M. Fairclough, L. M. Droessler, N. P. Young, J. H. Warner, J. M. Smith, H. E. Assender and A. A. R. Watt, *Chem. Commun.*, 2013, **15**, 3745-3747.
- J. Chang and E. R. Waclawik, *CrystEngComm*, 2013, **15**, 5612-5619.
- Zou, Y.; Su, X.; Jiang, J., *J. Am. Chem. Soc.* 2013, **135**, 18377-18384.
- A. Khare, A. W. Wills, L. M. Ammerman, D. J. Norris and E. S. Aydil, *Chem. Commun.*, 2011, **47**, 11721-11723.
- W. C. Liu, B. L. Guo, X. S. Wu, F. M. Zhang, C. L. Mak and K. H. Wong, *J. Mater. Chem. A*, 2013, **1**, 3182-3186.
- A.-J. Cheng, M. Manno, A. Khare, C. Leighton, S. A. Campbell and E. S. Aydil, *J. Vac. Sci. Technol. A*, 2011, **29**, 051203.
- X. Fontane, L. Calvo-Barrio, V. Izquierdo-Roca, E. Saucedo, A. Perez-Rodriguez, J. R. Morante, D. M. Berg, P. J. Dale and S. Siebentritt, *Appl. Phys. Lett.* 2011, **98**, 181905.

A graphical and textual abstract for the Table of contents entry



Facile and rapid one-pot synthesis for nearly monodisperse Cu₂SnS₃ and Cu₂ZnSnS₄ nanocrystals was developed, where their crystalline phase and size were simultaneously controlled by judiciously choosing the sulfur precursor reactivity and the oleic acid content.